A highly non-linear tellurite microstructure fiber with multi-ring holes for supercontinuum generation

Meisong Liao[a], Xin Yan, Guanshi Qin, Chitrarekha Chaudhari, Takenobu Suzuki, Yasutake Ohishi[b]

Research Center for Advanced Photon Technology, Toyota Technological Institute, 2-12-1, Hisakata, Tempaku, Nagoya 468-8511, Japan
[a]liaomeisong2005@yahoo.com.cn
[b]ohishi@toyota-ti.ac.jp

Abstract: We have fabricated a highly nonlinear complex microstructure tellurite fiber with a 1.8 micron core surrounded by four rings of holes. The cane for the fiber was prepared by combining the methods of cast rod in tube and stacking. In the process of fiber-drawing a positive pressure was pumped into the holes of cane to overcome the collapse of holes and reshape the microstructure. The correlations among pump pressure, hole size, surface tension and temperature gradient were investigated. The temperature gradient at the bottom of the preform's neck region was evaluated quantitatively by an indirect method. The chromatic dispersion of this fiber was compared with that of a step-index air-clad fiber. It was found that this fiber has a much more flattened chromatic dispersion. To the best of our knowledge this is the first report about a soft glass microstructure fiber which has such a small core together with four rings of holes for the dispersion engineering. The SC generation from this fiber was investigated under the pump of a 1557 nm femtosecond fiber laser. Infrared supercontinuum generation, free of fine structure, together with visible third harmonic generation was obtained under the pump of a femtosecond fiber laser with a pulse energy of several hundred pJ.

OCIS codes: (060.2280) Fiber design and fabrication; (190.0190) Nonlinear optics; (320.6629) Supercontinuum generation.

References and links

1. Y. S. Kivshar, "Nonlinear optics: the next decade," Opt. Express **16**(26), 22126–22128 (2008).
2. H. Takara, T. Ohara, K. Mori, K. Sato, E. Yamada, Y. Inoue, T. Shibata, M. Abe, T. Morioka, and K. I. Sato, "More than 1000 channel optical frequency chain generation from single supercontinuum source with 12.5 GHz channel spacing," Electron. Lett. **36**(25), 2089–2090 (2000).
3. A. F. Fercher, and E. Roth, "Ophthalmic laser interferometry," Proc. SPIE **658**, 48–51 (1986).
4. M. Nisoli, S. De Silvestri, and O. Svelto, "Generation of high energy 10 fs pulses by a new pulse compression technique," Appl. Phys. Lett. **68**(20), 2793–2795 (1996).
5. D. J. Jones, S. A. Diddams, J. K. Ranka, A. Stentz, R. S. Windeler, J. L. Hall, and S. T. Cundiff, "Carrier-envelope phase control of femtosecond mode-locked lasers and direct optical frequency synthesis," Science **288**(5466), 635–639 (2000).
6. H. Hundertmark, D. Kracht, D. Wandt, C. Fallnich, V. V. R. K. Kumar, A. K. George, J. C. Knight, and P. St. J. Russell, "Supercontinuum generation with 200 pJ laser pulses in an extruded SF6 fiber at 1560 nm," Opt. Express **11**(24), 3196–3201 (2003).
7. F. G. Omenetto, N. A. Wolchover, M. R. Wehner, M. Ross, A. Efimov, A. J. Taylor, V. V. R. K. Kumar, A. K. George, J. C. Knight, N. Y. Joly, and P. St. J. Russell, "Spectrally smooth supercontinuum from 350 nm to 3 μm in sub-centimeter lengths of soft-glass photonic crystal fibers," Opt. Express **14**(11), 4928–4934 (2006).
8. H. Ebendorff-Heidepriem, P. Petropoulos, S. Asimakis, V. Finazzi, R. C. Moore, K. Frampton, F. Koizumi, D. J. Richardson, and T. M. Monro, "Bismuth glass holey fibers with high nonlinearity," Opt. Express **12**(21), 5082–5087 (2004).

#114509 - $15.00 USD Received 20 Jul 2009; revised 1 Aug 2009; accepted 2 Aug 2009; published 17 Aug 2009

9. P. Domachuk, N. A. Wolchover, M. Cronin-Golomb, A. Wang, A. K. George, C. M. B. Cordeiro, J. C. Knight, and F. G. Omenetto, "Over 4000 nm bandwidth of mid-IR supercontinuum generation in sub-centimeter segments of highly nonlinear tellurite PCFs," Opt. Express **16**(10), 7161–7168 (2008).
10. X. Feng, W. H. Loh, J. C. Flanagan, A. Camerlingo, S. Dasgupta, P. Petropoulos, P. Horak, K. E. Frampton, N. M. White, J. H. V. Price, H. N. Rutt, and D. J. Richardson, "Single-mode tellurite glass holey fiber with extremely large mode area for infrared nonlinear applications," Opt. Express **16**(18), 13651–13656 (2008).
11. G. Qin, M. Liao, C. Chaudhari, Y. Arai, T. Suzuki, and Y. Ohishi, "Spectrum controlled supercontinuum generation in microstructure tellurite fibers," J. Cera. Soc. Jap. **117**(1365), 706–708 (2009).
12. M. Liao, C. Chaudhari, G. Qin, X. Yan, T. Suzuki, and Y. Ohishi, "Tellurite microstructure fibers with small hexagonal core for supercontinuum generation," Opt. Express **17**(14), 12174–12182 (2009).
13. C. M. B. Cordeiro, W. J. Wadsworth, T. A. Birks, and P. St. J. Russell, "Engineering the dispersion of tapered fibers for supercontinuum generation with a 1064 nm pump laser," Opt. Lett. **30**(15), 1980–1982 (2005).
14. G. Qin, X. Yan, C. Kito, M. Liao, C. Chaudhari, T. Suzuki, and Y. Ohishi, "Supercontinuum generation spanning over three octaves from UV to 3.85 μm in a fluoride fiber," Opt. Lett. **34**(13), 2015–2017 (2009).
15. J. J. Miret, E. Silvestre, and P. Andrés, "Octave-spanning ultraflat supercontinuum with soft-glass photonic crystal fibers," Opt. Express **17**(11), 9197–9203 (2009).
16. T. Hori, N. Nishizawa, T. Goto, and M. Yoshida, "Experimental and numerical analysis of widely broadened supercontinuum generation in highly nonlinear dispersion-shifted fiber with a femtosecond pulse," J. Opt. Soc. Am. B **21**, 1969–1980 (2004).
17. X. Feng, A. K. Mairaj, D. W. Hewak, and T. M. Monro, "Nonsilica glasses for holey fibers," J. Lightwave Technol. **23**(6), 2046–2054 (2005).
18. H. Ebendorff-Heidepriem, and T. M. Monro, "Extrusion of complex preforms for microstructured optical fibers," Opt. Express **15**(23), 15086–15092 (2007).
19. P. G. de Gennes, F. Brochard-Wyart, and D. Quere, "Capillary and Wetting Phenomena-Drops, Bubbles, Pearls, Waves," Springer. (2002).
20. W. Gregory H, "Statistical Physics," New York: Dover Publications. (1987).
21. A. N. Kensington, "The Physics and Chemistry of Surfaces, 3rd ed." Oxford University Press. (1941).
22. D. R. Austin, C. M. de Sterke, B. J. Eggleton, and T. G. Brown, "Dispersive wave blue-shift in supercontinuum generation," Opt. Express **14**(25), 11997–12007 (2006).
23. T. Schreiber, T. Andersen, D. Schimpf, J. Limpert, and A. Tünnermann, "Supercontinuum generation by femtosecond single and dual wavelength pumping in photonic crystal fibers with two zero dispersion wavelengths," Opt. Express **13**(23), 9556–9569 (2005).
24. M. Frosz, P. Falk, and O. Bang, "The role of the second zero-dispersion wavelength in generation of supercontinua and bright-bright soliton-pairs across the zero-dispersion wavelength," Opt. Express **13**(16), 6181–6192 (2005).
25. I. Cristiani, R. Tediosi, L. Tartara, and V. Degiorgio, "Dispersive wave generation by solitons in microstructured optical fibers," Opt. Express **12**(1), 124–135 (2004).
26. F. G. Omenetto, A. J. Taylor, M. D. Moores, J. Arriaga, J. C. Knight, W. J. Wadsworth, and P. S. J. Russell, "Simultaneous generation of spectrally distinct third harmonics in a photonic crystal fiber," Opt. Lett. **26**(15), 1158–1160 (2001).
27. A. Efimov, A. Taylor, F. Omenetto, J. Knight, W. Wadsworth, and P. Russell, "Phase-matched third harmonic generation in microstructured fibers," Opt. Express **11**(20), 2567–2576 (2003).
28. F. Poletti, and P. Horak, "Dynamics of femtosecond supercontinuum generation in multimode fibers," Opt. Express **17**(8), 6134–6147 (2009).

1. Introduction

Supercontinuum generation (SC) by photonic crystal fiber has had revolutionary impact on the development of nonlinear optics [1]. Applications of SC include multi-wavelength optical source for dense wavelength division multiplexing telecommunications [2], optical coherence tomography for medical imaging technique [3], pulse compression for ultrashort femtosecond laser source [4], and optical frequency metrology for the measurements of optical frequencies with unprecedented accuracy [5]. Highly nonlinear fiber is the prerequisite of a SC source composed of low-cost and compact devices. So far the rapid development of research on SC has benefited greatly from the technological maturity of silica glass photonic crystal fiber, which is characterized by a small core, and a chromatic dispersion which can almost be tailored freely. However, the nonlinear refractive index n_2 of silica glass is only 2.2×10^{-20} m^2/W, which is too low and restricts the further improvement of fiber nonlinearity. Additionally silica glass photonic crystal fiber is not transparent at the wavelengths longer than 3 μm, which makes the SC beyond this wavelength difficult. Nonsilica glasses such as tellurite glass and chalcogenide glass are transparent in the mid-infrared range, and have a n_2

#114509 - $15.00 USD Received 20 Jul 2009; revised 1 Aug 2009; accepted 2 Aug 2009; published 17 Aug 2009

higher than silica glass by at least one order of magnitude. Investigations on SC from these nonsilica glass microstructure fibers have already been reported in some papers lately [6–11]. Very recently we have fabricated a tellurte microstructure fiber with a 1 μm hexagonal core, and investigated the SC generated from it by a 1064 nm picosecond laser [12]. Nevertheless, so far the reported tellurite highly nonlinear small core fibers are the air-clad fibers. They almost have the similar microstructure, which is characterized by a small core surrounded by only one ring of air-holes. Such a simple microstructure provides a limited freedom of dispersion-engineering. Usually the chromatic dispersion of the fiber in this microstructure is not flattened enough because of the sharp contrast of refractive index between glass core and air-cladding [13].

For the SC generation pumped by ultrashort pulse, when the pump wavelength locates in the normal dispersion range, SC spectrum is broadened by self phase modulation (SPM) [14]. In this case a flattened dispersion contributes to the flatness and stability of SC greatly [15]. When the pump wavelength locates in the anomalous dispersion range, SC is mainly contributed by soliton propagation dynamics. The soliton number is resolved by:

$$N^2 = \frac{\gamma P_0 T_0^{\,2}}{|\beta_2|} \tag{1}$$

where γ is the nonlinear coefficient, P_0 is the peak power of pump pulse, T_0 is the width of pulse, and β_2 is group velocity dispersion (GVD). A higher value of N benefits the flatness of SC by eliminating the fine structure of spectrum. To get higher N at low peak power, β_2 is expected to be as low as possible. When the pump wavelength is close to the zero dispersion wavelength (ZDW), third order dispersion (TOD) has an important influence on the breadth of SC. A high TOD renders the splitting of pulse and reduces the spectrally broadening [16]. On the whole, a dispersion flattened fiber is preferable for a broad and flattened SC spectrum generated from a low-cost and compact device.

In order to obtain a flattened dispersion, a complex microstructure with multi-ring holes other than an air-cladding is necessary for the fiber. However, though dispersion flattened fibers by soft glass can be designed in various complex microstructures, the fabrication of them is still a challenge today [17]. By advanced techniques the preforms with complex microstructures might be prepared [18], but drawing it into fiber which can reproduce the microstructure is much more difficult. Firstly the viscosity of soft glass is very sensitive to temperature. It results a narrow temperature range of fiber-drawing. For example the temperature range of fiber-drawing for the tellurite glass is less than one-tenth that for the silica glass. In the fiber-drawing process the slightly temperature gradient across the profile of preform may induce obvious deformation of microstructure. Secondly because the thermal conductivity of air is less than that of glass by one order of magnitude, the air-holes disturb the even distribution of temperature field across the profile of the preform. For the highly nonlinear microstructure fibers the fabrication is even much more difficult. The core diameters of highly nonlinear fibers are small. It is usually in the size of from sub-micron to a few microns. For a microstructure fiber with multi-ring holes, such a small core usually is going with the holes which are also small. Because at fiber-drawing temperature the additional pressure, arising from surface tension, is converse to the hole size, the holes are subject to deformation or collapse even they are sealed. Additionally, the glass bridge between two holes is usually narrow for the small core fiber. Consequently the disturbance of air-holes to the thermal conduction gets much heavier than that for the large core fiber. Because of these difficulties, so far the report about soft glass fiber which has a small core surrounded by multi-ring holes is rare. In reference 10 the core diameter of the tellurite holey fiber, which has two ring holes, is 80 μm. In this paper, we have fabricated a complex microstructure fiber by tellurite glass which has a 1.8 μm core surrounded by four-ring holes. A positive pressure was pumped into the holes of preform in the fiber-drawing process to

#114509 - $15.00 USD Received 20 Jul 2009; revised 1 Aug 2009; accepted 2 Aug 2009; published 17 Aug 2009

overcome the collapse of holes and reshape the microstructure. The temperature gradient of the profile at the bottom of preform was analyzed. An indirect method was proposed to evaluate the temperature gradient quantitatively. The chromatic dispersion of this fiber was compared with that of an air-clad fiber. Furthermore the SC generation from this fiber was investigated by the pump of a femtosecond fiber laser.

2. Fiber fabrication and characterization

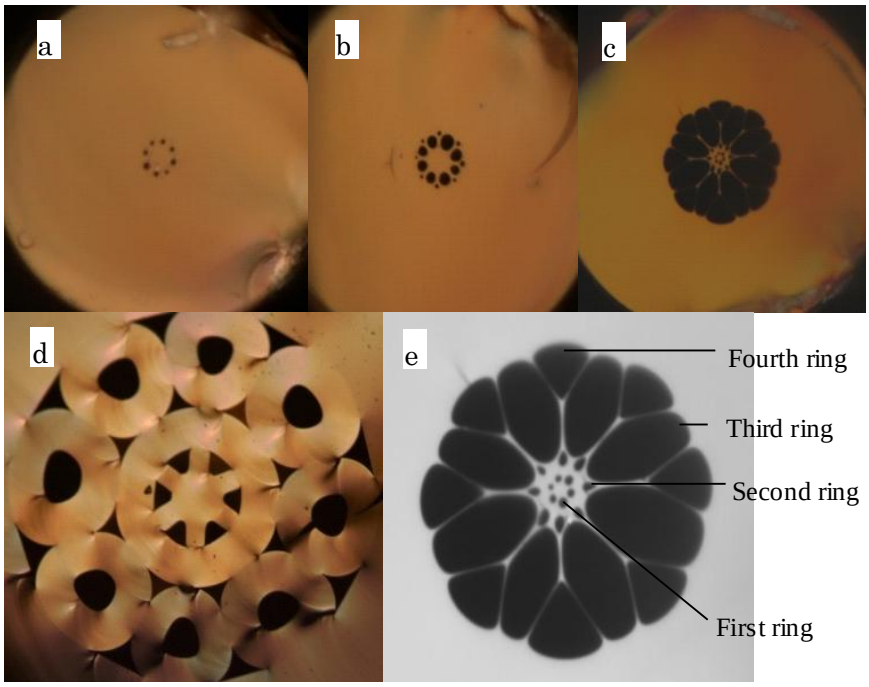

Fig. 1. The cross-sections of the fibers drawn under different pump pressures and the finial cane: a. 2.8 kPa; b. 3.6 kPa; c. 8.5 kPa; d. finial cane; e. 8.5 kPa. Inset a-d were taken by an optical microscope. Inset e was taken by a scanning electron microscope.

Nowadays the fabrication techniques for the preform include extrusion, cast rod in tube, ultrasonic drilling and stacking. The extrusion method requires equipment with high cost. Meanwhile the surface of holes is subject to contamination by the die. The cast rod in tube method is suitable for the simple structure, especially for the air-clad structure. Ultrasonic drilling requires both expensive equipments and long working time. Stacking method can manufacture fiber with highly complex microstructure, but it involves high human labor. In this research, we fabricated the cane by combing the methods of cast rod in tube and stacking. The composition of tellurite glass was $76.5TeO_2$-$6Bi_2O_3$-6ZnO-$11.5Li_2O$ (mol%). The raw materials were analytic grade. A tellurite glass rod in the shape of hexagon was prepared by casting the glass melt in an alloy mold and then annealing it at the transition temperature. The tellurite glass tubes were prepared by the rotational casting method. The rod was inserted into a tube and then was elongated into the original cane. Tellurite glass capillaries were prepared by elongating the tubes. Eight capillaries together with the original cane were stacked into another tellurite glass tube. The original cane was at the center surrounded by other eight capillaries which formed a ring. The tube stacked by original cane and capillaries was elongated into the final cane with the diameter of 2.5 mm. The final cane was inserted into another tellurite jacket tube, and then was fixed at the drawing tower for the fiber-drawing. The jacket tube was used to decrease the ratio of the core to cladding size. In the fiber-drawing process a positive pressure of nitrogen gas was pumped into the holes of the cane. In

#114509 - $15.00 USD Received 20 Jul 2009; revised 1 Aug 2009; accepted 2 Aug 2009; published 17 Aug 2009

Fig. 1 the cross sections of the fibers and final cane are shown. Inset a, b and c correspond to the pump pressures of 2.8, 3.6 and 8.5 kPa respectively. The final cane is shown in inset d. The fiber shown in inset c is the desired fiber. Its specific characteristics are shown in inset e. It has a 1.8 μm hexagonal core surrounded by four rings of holes. From the inner ring to the outer ring, the holes of the first ring derived from the holes of original cane. The holes of the second ring derived from the gap holes formed by the sidewalls of capillaries and the original cane. The holes of the third ring derived from the holes of capillaries. The holes of the fourth ring derived from the gap holes formed by the sidewalls of capillaries and tube.

Without pump pressure the holes disappeared due to the additional pressure pointing to the center of the hole's profile. The correlation between additional pressure and surface tension can be explained according to the Young–Laplace equation [19]:

$$\Delta P = \sigma\left(\frac{1}{r_x}+\frac{1}{r_y}\right) \tag{2}$$

where △P is the additional pressure, σ is the surface tension, r_x and r_y are radii of curvature in each of the axes that are parallel to the surface. For the cylindrical surface, r_x is the radius of fiber hole. Here the radius of the hole which is not circular is represented by the radius of the circular one which has the same area. r_y is infinite. Equation (2) can be revised as:

$$\Delta P = \sigma\frac{1}{r} \tag{3}$$

In Eq. (3) r is the radius of hole in fiber. For a stable fiber-drawing process, supposed the proportion among the microstructures of preform could be reproduced accurately by the fiber, the hole size of fiber should be:

$$r_0 = \sqrt{\frac{S_p}{S_f}}R \tag{4}$$

In Eq. (4) R is the radius of hole in preform. r_0 is the reproductive size of fiber hole. S_f and S_p are the speeds of fiber-drawing and preform-decline respectively. Consequently Eq. (3) can be revised as:

$$\Delta P = \sigma\frac{1}{R}\sqrt{\frac{S_f}{S_p}} \tag{5}$$

For a stable fiber-drawing process, σ, S_f and S_p are constants. From Eq. (5) it can be found for a smaller preform hole, a larger pump pressure is required to counteract △P.

In Fig. 1 the third ring in the fiber derived from the ring with the largest holes in the final cane. When the pump pressure increased gradually, it appeared firstly at a pump pressure of 2.8 kPa. The fourth ring in the fiber corresponded to the ring with the second large holes in the final cane. It appeared secondly. The first and second rings corresponded to the rings in a small and similar hole size in the final cane. They appeared almost at the same pressure of 8.5 kPa at last. It is more than three times that of 2.8 kPa. According to Eq. (5) it seems unreasonable because for the final cane the radius of the third ring is only about two times that of the first ring. This can be explained by the variation of σ. σ depends on the temperature and rises with the decrease in temperature. Because the temperature for fiber-drawing was 295 °C, according to Wien's displacement law [20] most of the radiation energy from the heating elements locates at wavelength out of the transparent range of tellurite glass. The radiation energy was absorbed by the jacket tube glass and then was conducted to the center. The temperature gradient was formed along the radius of preform's profile (the

#114509 - $15.00 USD Received 20 Jul 2009; revised 1 Aug 2009; accepted 2 Aug 2009; published 17 Aug 2009

preform represents the jacket tube containing the final cane). The emergence of the third and fourth rings increased the temperature gradient. When the pump pressure increased the holes were enlarged and the glass bridges became slim, their disturbance to the thermal conduction increased.

It is inconvenient to measure the temperature gradient directly. Here an indirect method was proposed to evaluate it quantitatively. According to Eotvos rule the correlation between surface tension and temperature can be expressed by Eq. (6) [21]:

$$\sigma = \frac{k(T_c - T)}{V^{\frac{2}{3}}} \tag{6}$$

where V is the molar volume of that substance, T_c is the critical temperature where the surface tension is zero, and k, which is a constant valid for almost all substances, is 2.1×10^{-7} J/(K·mol$^{-2/3}$). According to Eq. (5) and Eq. (6) the temperature difference △T between two rings can be calculated by:

$$\Delta T = \left|\Delta P_i R_i - \Delta P_j R_j\right| \sqrt{\frac{S_p}{S_f}} \frac{V^{\frac{2}{3}}}{k} \tag{7}$$

In Eq. (7) the subscript means the specific ring. When drawing fiber the preform shrank and a neck region was formed. Here △T corresponds to the cross section at the bottom of neck region, namely the top cross section of the fiber region.

Because in inset d of Fig. 1 the holes of the first and third rings have a shape more circular than that of other rings, these two rings were chosen to calculate △T between them. R_1 was 25 μm and R_3 was 52 μm respectively. S_p/S_f was 10000. Accurate value of $\triangle P_i$ should be the pump pressure under which the radius of fiber hole is equal to the reproductive size r_0. However, when the holes in fiber appeared initially, their radii were very sensitive to the pump pressure. From Eq. (3) it can be seen that when the pump pressure is slightly higher than the additional pressure, the holes become larger. What's more, a larger hole corresponds to a smaller additional pressure. Consequently the holes became larger and larger, until the superabundant pressure was offset by the tension originated from plastic deformation. In inset a of Fig. 1 the average radius of holes is about 1.0 μm. In inset e the average radius of holes in the first ring is about 0.7 μm. Though both of them are higher than their reproductive sizes respectively, because of the super-sensitivity of hole size to pump pressure, it is reasonable to believe that the pump pressures, 2.8 kPa for the third ring and 8.5 kPa for the first ring, were very close to their accurate additional pressures respectively. The calculated △T is 3.1 °C.

It is necessary to point out that we could not use the hole radius of each ring shown in inset e of Fig. 1 to fit Eq. (3), because in this case the pump pressure not only counteracted the additional pressure but also reshaped the third and fourth rings to a large extant.

The fully vectorial finite difference method (FV-FDM) was used to calculate the wavelength dependent propagation constants from which the chromatic dispersion of the fundamental mode was calculated. The simulations were based on scanning electron microscope images. The results were shown in Fig. 2. The ZDW is 1390 nm. The chromatic dispersion of the fundamental mode in another step-index air-clad fiber by the same glass was shown in Fig. 2 for a comparison. Both fibers have the same core diameter of 1.8 μm. The TODs at ZDW are 0.443 ps/(nm^2×km) for the complex microstructure fiber and 1.053 ps/(nm^2×km) for the air-clad fiber respectively. On the whole the complex microstructure fiber has a chromatic dispersion more flattened than that of the air-clad fiber.

The optical loss spectrum for the fiber was measured by using the standard cutback measurement technique. A homemade femtosecond fiber laser with the peak wavelength at 1557 nm was connected with a single mode fiber (SMF) by a connector. Beam from the SMF

#114509 - $15.00 USD Received 20 Jul 2009; revised 1 Aug 2009; accepted 2 Aug 2009; published 17 Aug 2009

was collimated into parallel by a lens of 20×0.25 NA. The parallel beam was focused and coupled into the tellurite microstructure fiber by a lens of 40×0.47 NA. The output end of the fiber was mechanically spliced with a silica fiber cable with large mode field by using a butt-joint method. The other end of the fiber cable was connected with the optical spectrum analyzer. After the SC generation measurement, the femtosecond fiber laser was replaced by a white light source. The measured optical loss spectrum of the fiber is shown in Fig. 3. Because the raw materials used in fiber fabrication were analytic grade, the losses can be decreased greatly by improving the purity of them.

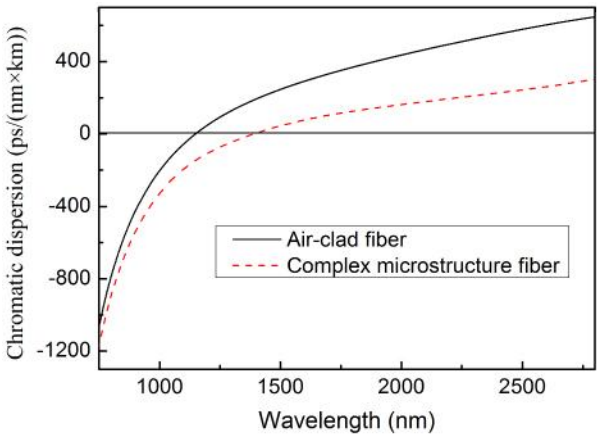

Fig. 2. Chromatic dispersion of the fundamental mode in the complex microstructure fiber. The chromatic dispersion of the fundamental mode in a step-index air-clad fiber is shown for a comparison.

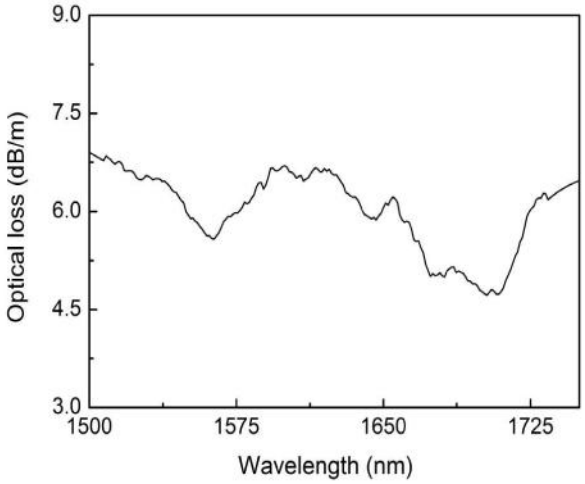

Fig. 3. Optical loss spectrum of the complex microstructure fiber measured by cut back method.

#114509 - $15.00 USD Received 20 Jul 2009; revised 1 Aug 2009; accepted 2 Aug 2009; published 17 Aug 2009

3. Supercontinuum generation

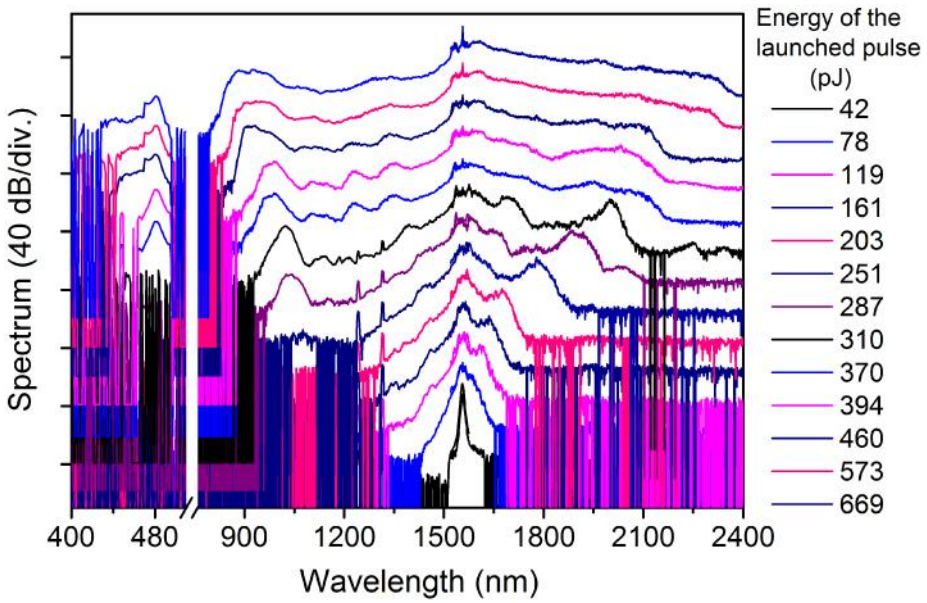

Fig. 4. Pulse energy dependent supercontinuum spectra of the complex microstructure fiber pumped by a femtosecond fiber laser. The curve is displaced by 20 dB.

Figure 4 shows the pulse energy dependent SC spectra measured by using a homemade femtosecond fiber laser at 1557 nm. The pulse width was 400 fs and the repetition rate was 16.75 MHz. The length of the microstructure fiber was around 30 cm. The small peaks at 1178 nm, 1245 nm and 1318 nm are CW parasitic multi-wavelength lasers from high power 1480 nm fiber Raman laser which is the pump source of the femtosecond fiber laser. The launched efficiency, defined as the launched power divided by the incident power on the lens, was about 10%. The nonlinear length L_{non} was calculated by: $L_{non}=1/(P_0\times\gamma)$. P_0 was defined in Eq. (1). γ is the nonlinear coefficient which can be calculated by:

$$\gamma = \frac{2\pi}{\lambda}\frac{\int\int_{-\infty}^{\infty} n_2(x,y)\left|F(x,y)\right|^4 dxdy}{(\int\int_{-\infty}^{\infty}\left|F(x,y)\right|^2 dxdy)^2} \tag{8}$$

In Eq. (8) $F(x,y)$ is the profile of the mode field. $n_2(x,y)$ is the distribution of nonlinear refractive index. It is 5.9×10^{-19} m^2/W for this tellurite glass, and 2.9×10^{-23} m^2/W for air. γ at 1557 nm is 394 $km^{-1}W^{-1}$. Under the maximal pulse energy the peak power of launched pulse is 1670 W. The nonlinear length is 1.5 mm which is much shorter than the effective length. Here we used the complex microstructure fiber in the length of 30 cm because this length was convenient for the experiment. The fiber length can be reduced greatly if required. The pump wavelength locates at the anomalous dispersion range. In this case the propagation dynamics of femtosecond pulse are already a well-known process. The soliton is generated by the combined effect of SPM and GVD. The order of soliton N calculated by Eq. (1) is 6 for the maximal pump power. The red-shift of SC ascribes to the soliton self-frequency shift, whose characteristic is clear for the SC spectra pumped by pulse with low energy.

The blue-shift of SC spectra except for the visible emission is due to the dispersive wave emitted in the process of fission of high order solitons. The wavelength of dispersive wave can be predicted by Eq. (9) [22–24]:

#114509 - $15.00 USD Received 20 Jul 2009; revised 1 Aug 2009; accepted 2 Aug 2009; published 17 Aug 2009

$$\sum_{n\geq 2}\frac{\beta_n(\omega_s)}{n!}(\omega_{DW}-\omega_s)^n=\frac{\gamma P_s}{2} \tag{9}$$

where ω_s and P_s are the soliton's centre frequency and peak power respectively, ω_{DW} is the frequency of dispersive wave, β_n is the n-th order derivative of the frequency-dependent wave vector. The calculated wavelength of dispersive waves λ_{DW} vs. the soliton's center wavelength λ_S are shown in Fig. 5. There is a close match between the SC spectra and the calculated phase matching condition considering that the practical value of λ_{DW} usually is a little lower than the calculated one because of the nonlinear phase shift [25].

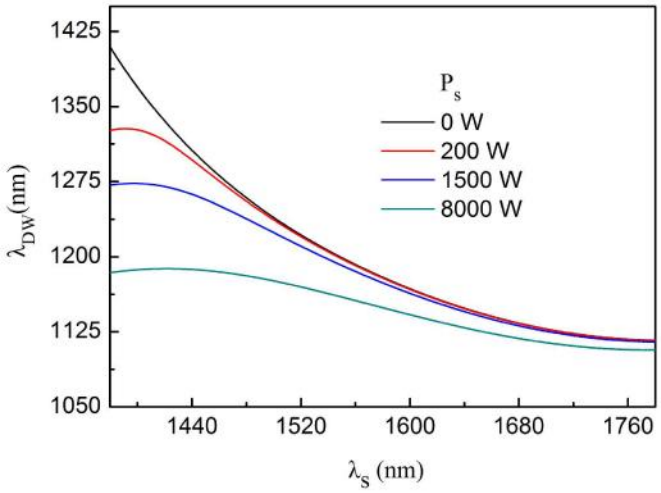

Fig. 5. Wavelength of dispersive waves λ_{DW} vs. the soliton center wavelength λ_S.

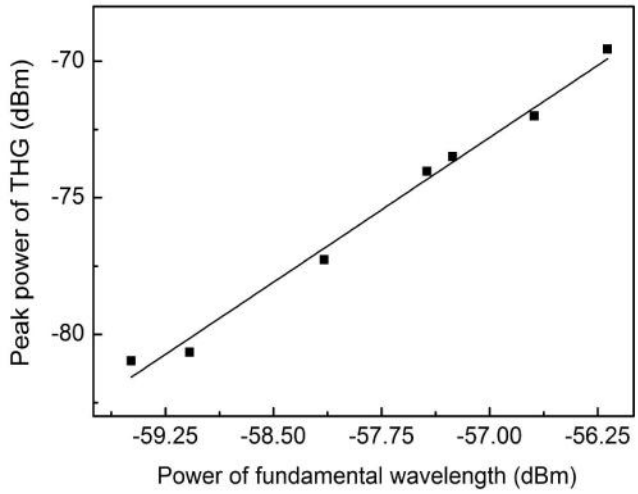

Fig. 6. Experimental peak power of the third harmonic signal as a function of the power of fundamental wavelength compared with a cubic fit shown by the straight line.

The visible emission peaked at 481 nm is the third harmonic generation (THG) of infrared emission [26,27]. Unlike the dispersive wave in the near-infrared, the peak wavelength of the visible emission shows no power dependence. In Fig. 6 it can be found the intensity of visible emission peak shows cubic power dependence on that of the fundamental wavelength.

According to the simulation for dispersion calculation, the fiber is not single mode at 1557 nm. It can support 4 modes. Probably there was intermodal energy transfer, and high order

#114509 - $15.00 USD Received 20 Jul 2009; revised 1 Aug 2009; accepted 2 Aug 2009; published 17 Aug 2009

modes might serve to extend the overall SC to the short wavelength [28]. Nevertheless, the SC spectra were stable, and could be repeated well when they were measured again. Due to the limitation of experiment conditions we have not observed other obvious evidence of non-single mode behavior in the experiment except for the visible harmonic generation.

The flatness and breadth of SC spectra were restrained by the pump power and the pump wavelength. The pump wavelength is too far away from the ZDW. However, under the maximal pump power the SC spectrum is already free of fine structure. The high nonlinearity together with flattened dispersion provides the possibility of broad and flat SC generated by the pump of all-fiber femtosecond laser. The pump pulse with the energy of several nJ or even higher is not necessary. Additionally the fiber loss is not a problem in this case because of the short nonlinear length. The harsh demands for the purity of raw materials and the fabrication conditions can be reduced greatly.

In reference 12, the tellurite microstructure fibers were pumped by the same femtosecond fiber laser. Because the normal dispersions in the range of shorter wavelength were too far from the pump wavelength, the dispersive wave was not observed at the wavelength shorter than 1557 nm. Additionally, since the nonlinear coefficients of those fibers are much higher than that of this complex microstructure fiber, the visible third harmonic generation is much more intense for these fibers except for the fiber SMF, which has a high confinement loss at the fundamental wavelength. In a word, a well engineered chromatic dispersion is important for the broad SC generation, and a high nonlinearity is important for the efficient third harmonic generation.

4. Summary

We have fabricated a complex microstructure tellurite fiber which has a 1.8 μm core surrounded by four ring holes. The preform was fabricated by the method of cast rod in tube and stacking. In the fiber-drawing process a positive pressure was pumped into the holes. The correlations among pump pressure, hole size, surface tension and temperature were investigated. An indirect method was proposed to evaluate the temperature gradient of the profile at the bottom of preform's neck region. It was shown that the design of dispersion flattened highly nonlinear fiber by soft glass must be a comprehensive work where the surface tension and thermal conduction in the process of fabrication need to be considered in advance.

For the soft glass holey fibers, if the hole-radius is in the magnitude of sub-micron, at fiber-drawing temperature the additional pressure due to surface tension will result in the deformation of microstructures, even though the holes of preform were sealed before fiber-drawing. So pumping a positive pressure into the holes in the fiber-drawing process is an important, probably a unique solution to this problem. In this paper the investigations on pump pressure, hole size and temperature gradient will serve as the guidance for the further development of this fabrication technique.

The complex microstructure fiber we have fabricated has a chromatic dispersion much more flattened than that of the step-index air-clad fiber. The SC generation from this fiber was investigated under the pump of a 1557 nm femtosecond fiber laser. Though the pump wavelength was far from the ZDW, infrared supercontinuum generation, free of fine structure, together with visible third harmonic generation was obtained under the pump of several hundred pJ pulse.

Acknowledgement

This work was supported by MEXT, the Private University High-Tech Research Center Program (2006-2010).

#114509 - $15.00 USD Received 20 Jul 2009; revised 1 Aug 2009; accepted 2 Aug 2009; published 17 Aug 2009